Towards Understanding the EEDF Variations in a Hall Thruster Channel due to Secondary Electron Emission in a Highly Controlled Crossed Field Experiment

IEPC-2013-398

Presented at the 33rd International Electric Propulsion Conference,
The George Washington University • Washington, D.C. • USA
October 6 – 10, 2013

Kapil U. Sawlani[1] and John E. Foster[2]
University of Michigan, Ann Arbor, MI, 48109, USA

Abstract: The role of secondary electron emission in Hall thruster has been a subject of considerable interest in recent times. Several computational and analytical efforts exist with very few supporting experimental efforts. This works attempts to investigate the influence of secondary electron emission in the presence of plasma in a basic cross field device possessing attributes similar to a Hall thruster. A detailed description of the apparatus is presented. Results from a preliminary operation of the apparatus is also presented. This paper also discusses methods that will be used in this effort to determine the variation in the plasma EEDF and plasma sheath profile near an insulating target as a function of electron beam irradiation used to stimulate SEE.

Acronyms

HET	=	Hall Effect Thruster
ESA	=	European Space Agency
SPT	=	Stationary Plasma Thruster
TAL	=	Thruster with Anode Layer
SEE	=	Secondary Electron Emission
EEDF	=	Electron Energy Distribution Function
OAF	=	Open Air Fraction

I. Introduction

HALL thrusters[1] are crossed field devices used for satellite station keeping and orbit transfer applications. They have also been employed for space exploration such as the ESA SMART-1 mission. The HET can be classified in many ways based on geometry and material used in the construction of the acceleration channel. The material used in the thruster acceleration channel plays a major role in its operation and based on it, the HET is usually categorized as an SPT (when the channel is constructed using a dielectric material) or TAL (when the channel wall is made of metal). The usual choice of material for a SPT channel wall is boron nitride (BN).

SEE induced by primary electron impact on the BN channel can drastically affect the energy distribution of the electrons, the sheath potential, cross-field current and heat flux to the walls[2-7]. Figure 1 shows the basic processes that take place when a wall is immersed in a plasma, along with sheath potential profile both in presence and absence of SEE.

[1] Graduate Student Research Assistant, Nuclear Engineering and Radiological Sciences, sawlanik@umich.edu.
[2] Assoc. Professor, Nuclear Engineering and Radiological Sciences, jefoster@umich.edu.

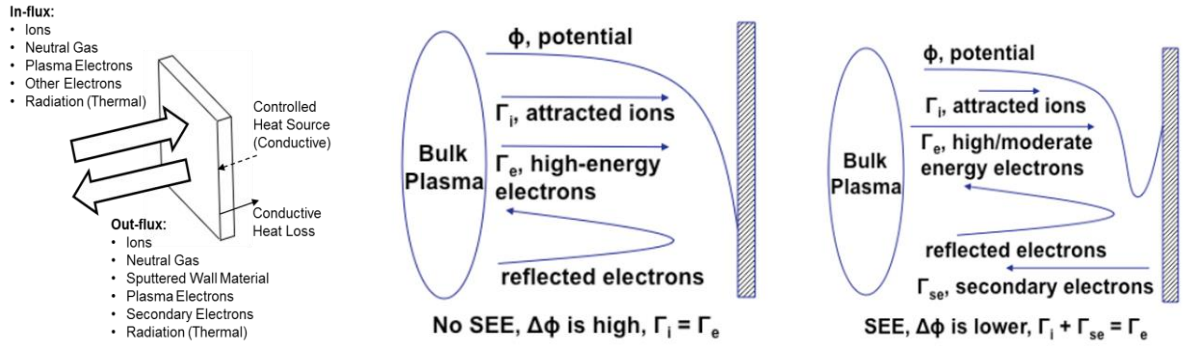

Figure 1. Plasma wall interaction. *Figure shows the basic processes that occur when a wall is immersed in a plasma. Also shown are the sheath potential profiles in the limit of no SEE and when there is a finite SEE from the wall.*

The role of SEE in the operation of a Hall thruster has been a subject of investigation in the recent past. The interaction of energetic electrons with the channel wall produce secondary electrons that can have a non-linear coupling effect with the bulk plasma and affect the performance of crossed field devices. However, this influence is not yet fully understood in the community. Experimentally, there is no available data on the SEE yield in the presence of a plasma, which could be used to validate existing numerical models. Thus needed is a test-bed apparatus that could serve as a tool to validate and improve existing numerical models by providing the appropriate boundary conditions, secondary yield coefficients and variation of plasma parameters to aid future design of Hall thrusters.

Presented here is the status of such a crossed field bench-top test facility designed to study the effects of controlled electron bombardment on ceramic targets in the presence of a low density (10^7 cm^{-3} to 10^8 cm^{-3}). The associated thick sheath at the BN target affords one the opportunity to resolve potential spatial distribution changes in response to irradiation by electron beams. Changes in the electron energy distribution function in response to induced SEE are to be tracked using a Langmuir probe. The goal is to characterize the sensitivity of these changes to cross-field magnetic field strength. These findings coupled with spatially resolved emissive probe measurements in the thick sheath of the electron beam irradiated, ceramic target will allow us to characterize completely the influence of SEE in Hall thruster plasma. Utilization of the data obtained from this work will ultimately be used for the purpose of model validation and boundary condition establishment, which would aid in future Hall thruster design codes.

II. Experimental Apparatus

The experiment consists of a bench-top system designed to simulate the conditions similar to that seen a typical Hall thruster. The current apparatus eliminates the complexity of phenomena encountered in real devices such as rotating spokes and oscillating (breathing) modes. Existing literature indicates the difficulty of understanding the effects of these phenomena, which occur under different operation conditions. The isolation of physics using the

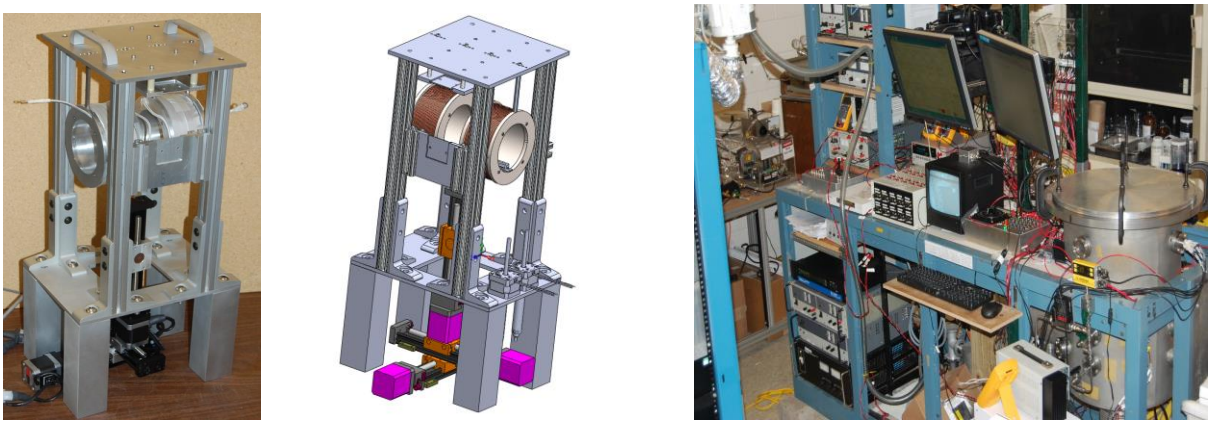

Figure 2. Experimental Facility and Components. *Figure shows the main experimental bench-top apparatus along with its 3D model. Also shown is the experimental system with associated power supplies and other systems required for monitoring and control.*

bench-top facility suggested here would account purely for secondary electron emission effects to the bulk plasma properties as well as variation within the sheath. This isolation is accomplished by operating various subsystems, described in this section, to simulate the conditions encountered in a region closer to the walls of the acceleration channel. Figure 2 shows the experimental bench top facility along with its 3D model used in this study. Also shown in the figure is the complete experimental system.

A. Electromagnets

The applied field is simulated using the Helmholtz coil arrangement. In such an arrangement the radius of the magnet spool is equal to the length between the two spools. In this system, R = L = 5.08 cm. The copper wire used for winding the magnet is AWG 12 and a total of 120 ± 5 turns (5 layers of 24 ± 1 turns) are given to each spool. Figure 3 shows the 3D model of the electromagnets attached to the top plate and also provides magnetic maps for few current conditions. This is compared with results from commercial MAXWELL solver results.

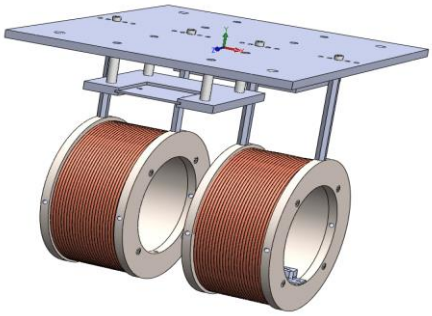

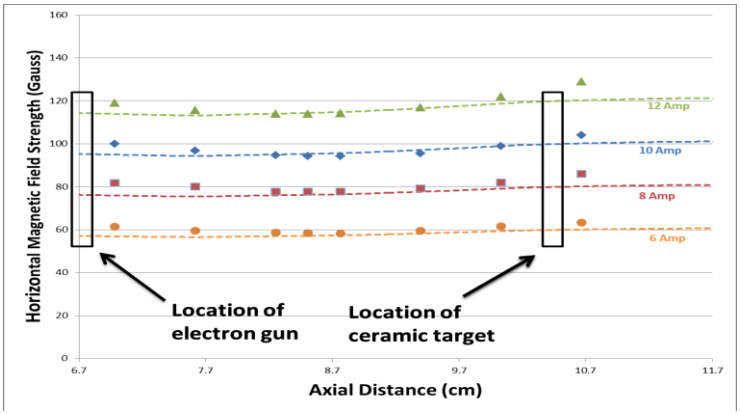

Figure 3. Electromagnets and Magnetic Field Map. *Figure shows 3D model for electromagnet and a demonstrative magnetic map compared with simulations. Dotted lines correspond to simulation results.*

The electromagnet has been tested up to 200 Gauss. The system is also capable of producing non-uniform magnetic topologies by applying different currents on each magnet spool.

B. Low Energy Electron Gun

A low energy electron gun, which is used as a source of primary electrons was designed and constructed from stainless steel. The 2.54 cm diameter electron gun has been tested with several grids of transparencies ranging from approximately 18% OAF to approximately 79% OAF. The emitting filament is made from a 1% thoriated tungsten (1-Th-99-W) and coated with a barium-strontium-calcium carbonate [(Ba-Sr-Ca)CO_3 56-31-13%]. Figure 4 shows the electron gun with a high transparency grid along with its 3D model.

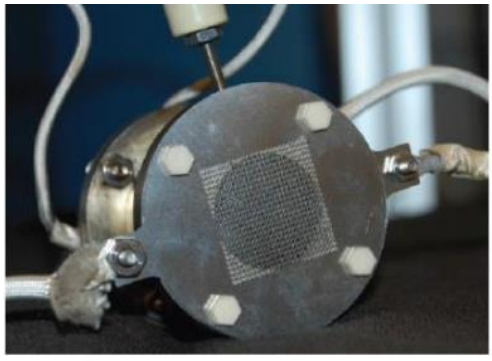

Figure 4. Electron Gun. *Figure shows an electron gun with high transparency grid used for SEE tests along with a 3D model*

The electron gun has been designed and characterized to produce a 1mA electron beam to irradiate the ceramic target. The goal of this experiment is to operate at conditions where the electron flux to the insulator due to the plasma alone is at least an order of magnitude below the deposited beam current, i.e., at densities of 10^7 cm^{-3} to 10^8 cm^{-3}. This excess electron beam current in comparison to the plasma current density would allow for good signal to noise ratio. Figure 5 shows a typical curve from electron gun current with variation in the magnetic field. Considerable effort is being taken to minimize the effect of magnetic fields within the electron gun using shielding metal.

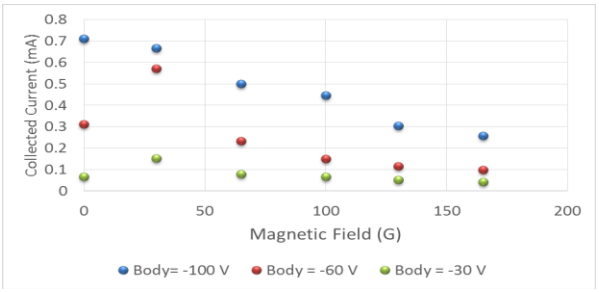

Figure 5. Electron Gun Emission Current. *Figure shows a typical electron gun emission current curve as a function of magnetic field with varying body bias.*

C. Target (Wall Material)

Several materials will be investigated for SEE and its effect on plasma behavior. These include~~s~~, various grades of Boron Nitride [Grade A Combat, Grade AX05 Combat, Grade HP Combat, Grade M Combat, and Grade ZSBN Combat], Alumina, Aluminum and Graphite. Of particular interest are the different grades of BN products which have very different crystal structure based on machining direction. Different surface roughness and crystal orientation, mainly of BN will be tested and characterized as they are most commonly used in Hall thrusters. Comparison of these data with graphite (electron absorbing surface) targets would provide useful insight into the importance of SEE on local plasma properties. All target materials will be pre- and post-characterized using a stylus profilometer, SEM images and XPS for surface/chemical characterization. The targets are fabricated to include several flush mounted probes as discussed in section II E.

D. Crossed Field Plasma Discharge

In order to generate a crossed field discharge plasma, two filaments cathodes were implemented. The thoriated tungsten filaments were coated with a low work function material of similar composition to the electron gun cathode. The geometry of the filaments is such that the electrons have to cross the axial magnetic field to reach the anode plate. Discharge is operated in constant current mode over a current range from 10's of mA to 100's of mA. Discharge characterization measurements are discussed in section III.

E. Experimental Diagnostics (Electrostatic Probes)[8]

Electrostatic probes are used to determine plasma parameters, sheath potential profile and EEDF in response to electron beam irradiation of the target. Figure 6 shows the various probes utilized in this experiment.

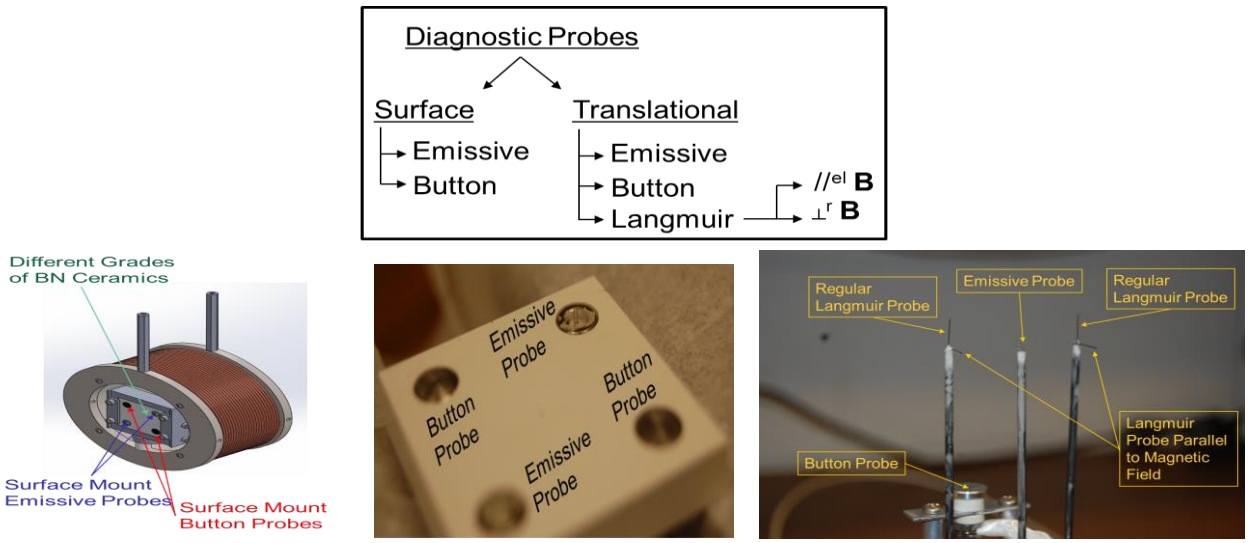

Figure 6. Electrostatic Probe Diagnostics. *Figure shows various methods used to determine the SEE effects in plasma.*

1. *Emissive Probes*

Emissive probes are used to assess the shape and potential distribution at the insulator target as well as measure the voltage drop across the simulated channel magnetic field. The presence of these probes on the surface provide a way to measure repeatability under the given circumstances. The insulating target also contains emissive probes to determine the potential very near the insulating target surface. This set of probes should allow for the detection of the virtual cathode if present as well. The resolution of the motion control system used to position the probes is 0.0025 mm. The plasma potential is measured using the floating point method and verified by the inflection point in the limit of zero emission method. These methods are described in ref. 9 and other references therein.

2. *Button Probes*

Flush mounted button probes on the surface of the target (approximately 6.8 mm in diameter) is used measure the flux of incident primary electron beam to the surface.

3. *Langmuir Probes*

Langmuir probes cannot be used within the sheath. They are mainly used to determine plasma parameters in the bulk plasma. Two probe orientations are utilized in this work. The probes are oriented perpendicularly and parallel to the magnetic field to assess flow and magnetic effects. The second derivative of the probes I-V characteristic allows for the determination of the EEDF[10, 11] in response to electron irradiation of the target.

The probe holder for all probes is made out of alumina. In order to minimize the contribution to SEE produced by electron bombardment of this ceramic, the probe holder body is coated with an SEE suppressing coating.

III. Results, Discussion, and Future Work

Figure 7 shows the plasma source under operation. The discharge currents shown here range from 15mA to 250mA. Over the discharge currents investigated and shown in figure 8, plasma density ranged in the order from 10^7 to 10^9 cm^{-3}. The low plasma densities are associated with the thick sheath conditions amenable to emissive probe measurements.

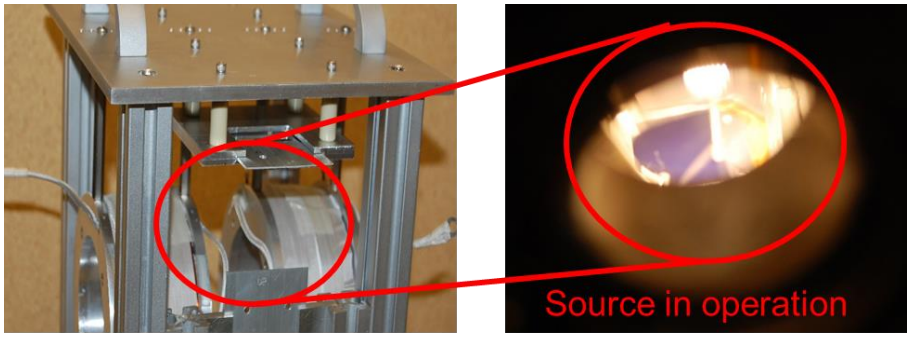

Figure 7. Crossed Field Discharge. *Figure shows a crossed field discharge.*

As seen in figure 8, the required voltage to maintain a given cross-field current increases with increasing magnetic field. This variation is directly related to reduction in cross field diffusion due to the presence of the magnetic field; that is, the cross field impedance increases as expected with increasing magnetic field strength.

Langmuir probes will be used to determine the EEDF using the Druvyesteyn method given by Eq. 1:

$$f(E) = \frac{2m_e}{e^2 A_p}\left(\frac{2e}{m_e}\right)^{\frac{1}{2}} \sqrt{E}\,\frac{d^2 I_{pr}}{dV_{pr}^2} \tag{1}$$

where $E = V_{plasma} - V_{probe}$

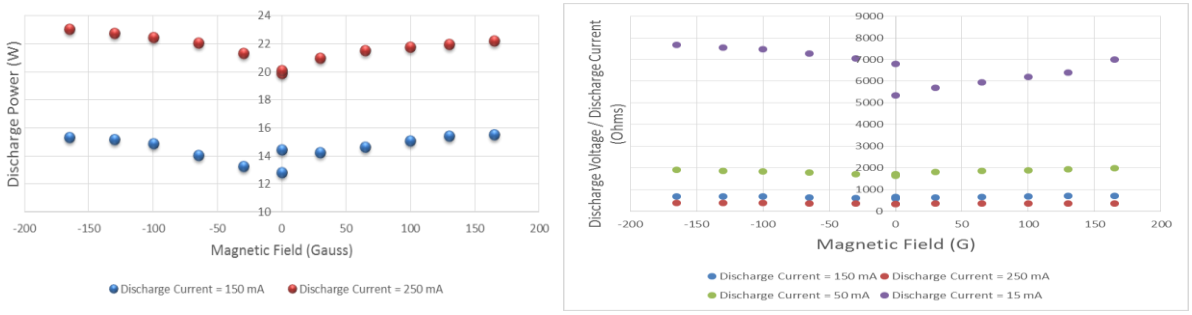

Figure 8. Crossed Field Power and Impedance Variation. *Figure shows increasing impedance and power with increasing magnetic field, a consequence of crossed field device operation.*

Determination of this EEDF can be challenging at the anticipated low plasma densities. Several numerical techniques discussed in ref. 12 have been used by the authors to effectively smooth out the noise. However, care will be taken not to lose essential physics as SEE effects might be incorporated in the noise and that information needs to be preserved.

SEE yield is also a function of angle of incidence of the primary electrons, temperature of the wall surface, grade and crystal orientation of the material, as well as surface roughness. These parameters therefore also influence the behavior of plasma sheath and bulk plasma. To date, the dependence of SEE on these parameters have only been characterized in a vacuum environment. The bench-top facility was designed specifically to determine the dependence of SEE effects on these parameters as well. Figure 9 illustrates the methods implemented to determine the effect of impact angle and surface temperature of the wall material on the secondary electron yield and corresponding plasma properties changes. Various grades and crystal structures of BN samples are available and fabricated to accommodate surface mount probes as described in section II (E). These samples would be characterized before and after experiments using a stylus profilometer, SEM, and XPS to understand the surface roughness, crystal orientation and material composition. All samples of the same type will have different surface roughness. As described in ref. 13, the surface roughness is an important parameter and changes from its pristine state following channel fabrication to a rough surface after several hours of operation, and the roughness values at different planes of the channel are not constant. These studies will complement the existing effort on mapping sheath profile variation and EEDF variations due to SEE.

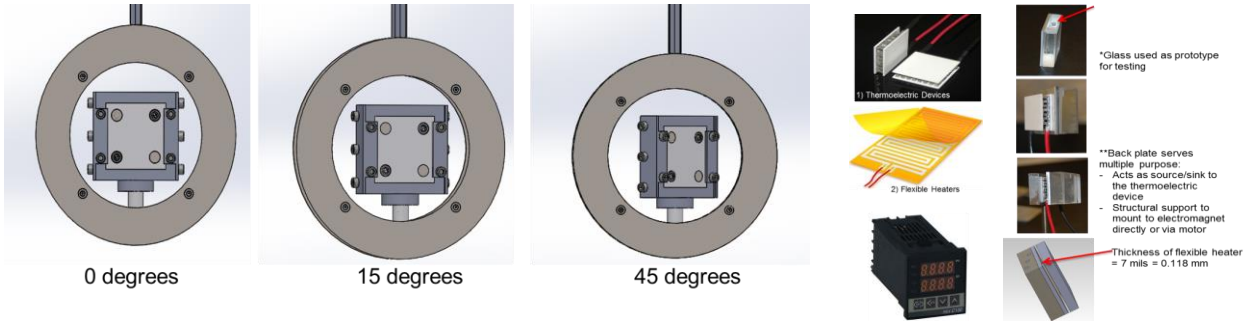

Figure 9. Impact Angle and Temperature. *Figure shows how the impact angle of the primary with respect to the target can be varied for a few demonstrative angles. Also shown are the devices available to control temperature of the target material.*

IV. Conclusion

A bench-top apparatus has been designed and fabricated to study the effects of secondary electron emission driven by an applied low energy electron beam in the presence of a discharge plasma and applied magnetic field. The system is nominally operated at low plasma density to produce thick sheaths amenable to emissive probing. The electron beam generated using a low energy electron gun far exceeds the floating current that would be encountered by the probes which provides a good SNR. A wide variety of diagnostic suite has been designed to study the effects

of SEE. The apparatus is also capable of elucidating effects such as e-beam impact angle, target surface, and grade/orientation on the SEE-driven plasma response.

Acknowledgments

The authors would like to acknowledge the funding support from Air Force Office of Scientific Research (AFOSR) under the grant FA9550-09-1-0695. K. U. Sawlani would like to thank Saint Gobain ceramic material division for providing BN samples used in these experiments.

References

[1]Goebel, M., D., and Katz, I., *Fundamentals of Electric Propulsion: Ion and Hall Thrusters*, 1st ed., Wiley and Sons, 2008.

[2]Hobbs, G. D., and Wesson, J. A., "Heat Transmission through a Langmuir Sheath in the Presence of Electron Emission," *Technical Report Culham Lab*, June 01 1966.

[3]Raitses, Y., Kaganovich, D., Khrabrov, A., Sydorenko, D., Fisch, N. J., and Smolyakov, A., "Effects of Secondary Electron Emission in Electron Cross-field Current in E x B Discharges," *IEEE Trans on Plasma Science*, 39, 4, April 2011, pp. 995, 1006

[4]Schwager, L. A., "Effects of Secondary and Thermionic Electron Emission on the Collector and Source Sheaths of a Finite Ion Temperature Plasma Using Kinetic Theory and Numerical Simulation," *Phys. Fluids B*, 5, 1992, pp. 631

[5]Taccogna, F., Longo, S., and Capitelli, M. "Plasma-Surface Interaction Model with Secondary Electron Emission Effects," *Phys of Plasmas*,11, 2004, pp. 1220

[6]Ahedo, E., Pablo, V., and Martinez-Sanchez, M. "Effects of Partial Thermalization and Secondary Emission on the Electron Distribution Function in Hall Thrusters," *IEPC – 2005 - 118*, 2005

[7]Sydorenko, D., Smolyakov, A., Kaganovich, I., and Raitses, Y., "Kinetic Simulation of Secondary Electron Emission Effects in Hall Thrusters," *Phys of Plasmas*,13, 2006, pp. 014501-1, 014501-4

[8]Chen, F. F., *Chapter 4: Electric Probes, Plasma Diagnostic Techniques*, edited by R. H. Huddlestone and S. L. Leonard, Academic Press, New York, 1965, pp. 113-200.

[9]Sheehan, J. P., Raitses, Y., Hershkowitz, N., Kaganovich, I., and Fisch, N. J., "A Comparison of Emissive Probe Techniques for Electric Potential Measurements in a Complex Plasma," *Phys of Plasmas*,18, 2011, pp. 073501-1, 073501-9

[10]Druyvesteyn, M. J., "Der Niedervoltbogen," *Zeitschrift für Physik*, Vol. 64, July 1930, pp. 781-798.

[11]Popov, T. K., Ivanova, P., Dimitrova, M., Kovacic, J., Gyergyek, T. and Cerek, M., "Langmuir Probe Measurement of the Electron Energy Distribution Function in Magnetized Gas Discharge Plasma," *Plasma Sources Science and Technology*, 21, 2, 2012, 025004

[12]Sawlani, K. U., and Foster, J. E., "Comparison of Various Numerical Schemes to Obtain EEDF with High Accuracy," *IEPC – 2009 - 043*, 2009

[13]Zidar, D. G., and Rovey, J. L., "Hall-Effect Thruster Channel Surface Properties Investigation," *AIAA Journal of Power and Propulsion*, Vol. 28, No. 2, March-April 2012, pp. 334, 343.